Pharmaceutical Research (2022) 39:2305–2314
https://doi.org/10.1007/s11095-022-03326-7

ORIGINAL ARTICLE

Modulation of Solid-State Chemical Stability of Gabapentin by Pyridinecarboxylic Acid

Minshan Guo[1] · Xiaojie Sun[1] · Shaozheng Zhang[1] · Ting Cai[1]

Received: 17 May 2022 / Accepted: 27 June 2022 / Published online: 7 July 2022

Abstract

Purpose Gabapentin (GBP) is an anticonvulsant drug with poor chemical stability that is particularly sensitive to heat and mechanical stress, which can lead to intramolecular lactamization. The purpose of this study was to enhance the chemical stability of GBP by cocrystallization with organic acids.

Method Two novel multicomponent crystals, GBP-2,6-pyridinedicarboxylic acid salt (GBP-2,6PDA salt) and GBP-2,5-pyridinedicarboxylic acid cocrystal (GBP-2,5PDA cocrystal) were synthesized and characterized by various solid-state analytical techniques. The degradation behavior of GBP, GBP-2,6PDA salt and GBP-2,5PDA cocrystals were evaluated under thermal and mechanical stresses.

Result Under thermal and mechanical stresses, GBP-2,5PDA cocrystals were found to undergo severer degradation than GBP-2,6PDA salt and neat GBP. GBP-2,6PDA salt exhibited superior chemical stability compared to the others. Furthermore, the crystal structure revealed that the order of atomic distance between the carboxyl group (C7) and amino group (N12) of GBP is as follows: GBP-2,5PDA cocrystal < GBP < GBP-2,6PDA salt, which is consistent with the chemical stability of GBP in different solid forms. Therefore, we believe that the distance between C7 and N12, the reaction active sites leading to dehydrative condensation of GBP, is a key factor determining the chemical stability of GBP in the solid state.

Conclusions These results provide a potential method to improve the chemical stability of GBP during the manufacturing process and storage.

Keywords Gabapentin · Crystal engineering · Chemical stability · Thermal stress · Mechanical stress

Introduction

Gabapentin (GBP, 1-(aminomethyl) cyclohexane acetic acid, a γ-aminobutyric acid (GABA) analog), is used for the treatment of epilepsy, postherpetic neuralgia, and seizures [1, 2], and was discovered in 1993 [3]. In contrast to GABA, GBP readily passes the blood–brain barrier because of its lipophilic characteristic [4], leading to a high concentration of GBP in the central nervous system for controlling seizures [5]. Moreover, GBP is the first-line therapy for neuropathic pain management in spinal cord injury, post therapeutic neuralgia and diabetic neuropathy [6–8]. However, owing to its inherent structural features, GBP suffers from chemical degradation during storage and manufacturing processes (such as milling, granulation and thermal treatment) [9–12]. The major chemical degradation pathway of GBP is lactamization to form gabapentin-lactam (gaba-L) via an intramolecular condensation between the amine and the carboxlylate acid (Scheme 1) [13]. Previous studies showed that gabapentin-lactam is more toxic than GBP [13–15]. USP40-NF35 stipulates that the content of degradant Gaba-L in GBP tablets and powder should be lower than 0.4% and 0.1% (w/w), respectively [12]. Hence, improving the chemical stability of GBP during the manufacturing process is important to ensure the potency and safety of the product for clinical use.

Crystal engineering of pharmaceutical solids is a versatile and effective strategy to modulate the physicochemical properties of active pharmaceutical ingredients (APIs) including hygroscopicity, solubility, bioavailability and compressibility [16, 17]. Several recent studies employed

Minshan Guo and Xiaojie Sun contributed equally to this work.

✉ Ting Cai
tcai@cpu.edu.cn

[1] State Key Laboratory of Natural Medicines, Department of Pharmaceutics, College of Pharmacy, China Pharmaceutical University, Nanjing 210009, China

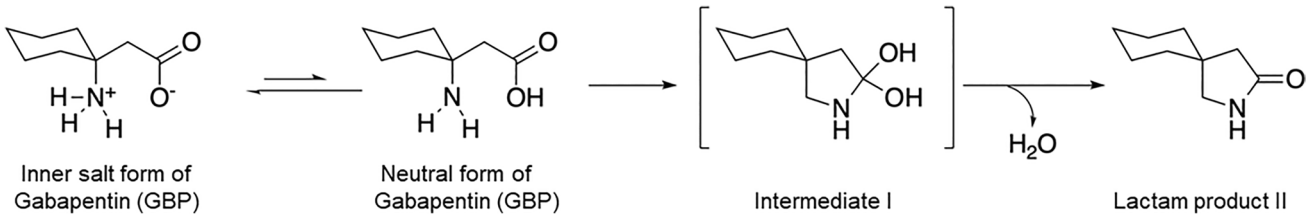

Scheme 1 Molecular structure of gabapentin and lactamization process.

crystal engineering to address the stability deficit of chemically unstable drugs such as vitamins, nifedipine and emodin [18–20]. For instance, the photodegradation of nifedipine was significantly inhibited via cocrystallization with isonicotinamide, owing to an extended distance between the reaction sites of nifedipine after the introduction of isonicotinamide [20]. In addition, the vitamin D_3 cocrystal with cholesterol also exhibited superior chemical stability compared with vitamin D_3 alone as a result of the high crystallinity and denser layer structure of the cocrystal [18]. Mei and coworkers summarized that the underlying mechanism behind the modified solid-state stability by crystal engineering includes alteration of interaction strength, conformation in the solid-state, packing styles and charge transfer or redistribution [21].

The crystal structures of multicomponent crystals of GBP with a series of carboxylic acids have been reported and included in the Cambridge Structural Database (CSD) [22, 23]. The desirable supramolecular synthons related to the GBP multicomponent mostly tend to form carboxylate-carboxylate, ammonium-carboxylate and hydroxy- carboxylate interactions [22]. Herein, two pyridinecarboxylic acid isomers, 2,6-pyridinedicarboxylic acid (2,6-PDA) and 2,5-pyridinedicarboxylic acid (2,5-PDA), were selected as the coformers (Scheme 2). The corresponding GBP-2,6PDA salt and GBP-2,5PDA cocrystals were synthesized and characterized by various solid-state analytical techniques. Compared to the neat GBP and GBP-2,5PDA cocrystals, the GBP-2,6PDA salt exhibited distinct chemical stability under thermal and mechanical stresses.

Materials and Methods

Materials

Gabapentin form II, 2,6-pyridinedicarboxylic acid and 2,5-pyridinedicarboxylic acid were purchased from Aladdin Biochemical Technology Co., Ltd. (Shanghai, China), with a purity greater than 98%. Methanol and ethanol were obtained from Tedia Company, Inc. (Anhui, China) and Shanghai Titan Scientific Co., Ltd. (Shanghai, China), respectively. All reagents were used as received without further purification.

Synthesis and Characterization

GBP-2,6PDA Salt

A bulk powder sample of GBP-2,6PDA salt was synthesized by slurry methods. GBP (34.2 g) and 2,6-PDA (33.4 g) in a 1:1 molar ratio were suspended in ethanol and stirred at room temperature for 3 days. The resultant suspension was then filtered and the residual solids were dried under vacuum at 40°C for 24 h.

For cultivate the single crystals of GBP-2,6-PDA salt, a mixture of GBP (85.5 mg) and 2,6-PDA (83.5 mg) was completely dissolved in ethanol (30 mL) and the solution was filtered through a 0.45 μm microfiltration membrane. Subsequently, the solution was slowly evaporated for 3 days at ambient temperature, yielding colorless prismatic crystals.

Scheme 2 Chemical structures of 2,6-pyridinedicarboxylic acid (2,6-PDA) and 2,5-pyridinedicarboxylic acid (2,5-PDA).

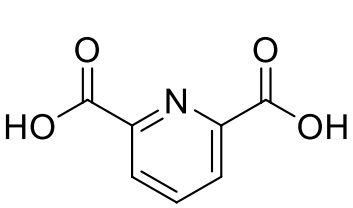

2,6-pyridinedicarboxylic acid

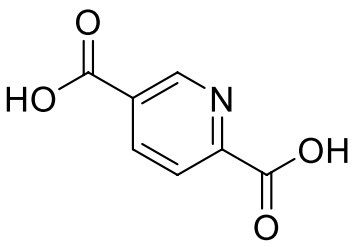

2,5-pyridinedicarboxylic acid

GBP-2,5PDA Cocrystals

Bulk powder of GBP-2,5PDA cocrystals was synthesized by the solvent evaporation method. A 1:1 stoichiometric ratio of GBP (34.2 g) and 2,5-PDA (33.4 g) was dissolved into 500 mL of methanol, and the resulting solution was allowed to evaporate at room temperature for 3 days. The cocrystal powder was then collected and dried at 40°C for 24 h. A high-quality single crystal of the GBP-2,5PDA cocrystal was harvested by slow evaporation of the methanol solution for 5 days at room temperature.

Differential Scanning Calorimetry (DSC)

Differential scanning calorimetry experiments were carried out using a DSC TA Q2000 instrument under a nitrogen gas flow of 50 mL/min purge. The temperature and heat flow were calibrated using standard indium. Approximately 2–4 mg of powder sample was heated in a sealed aluminum pan from 40℃ to the desired temperature at a heating rate of 3℃/min.

Thermogravimetric Analysis (TGA)

Thermogravimetric analysis was performed on TA Q500 thermogravimetric analysis equipment. The sample was heated from room temperature to 400℃ at a heating rate of 10℃/min. Nitrogen was used as the purge gas at 60 mL/min.

Powder X-ray Diffraction (PXRD)

PXRD patterns were obtained on a D8 Advanced X-ray diffractometer (Bruker, Germany) using Cu Kα radiation (λ = 1.5406 Å). The tube voltage and current of the generator were set to 40.0 kV and 40.0 mA, respectively. The data were acquired over a range of 3–40°(2θ) in continuous scan mode with a 0.02°(2θ) step size and 1 s step time.

Single Crystal X-ray Diffraction Analysis (SCXRD)

The single crystal X-ray diffraction of GBP-2,6PDA salt ($0.16 \times 0.12 \times 0.08$ mm^3) and GBP-2,5PDA cocrystal ($0.18 \times 0.15 \times 0.12$ mm^3) was conducted on a Bruker D8 Venture diffractometer with Mo Kα radiation (λ = 0.71073 Å). Data collection, cell refinement and data reduction were completed by Bruker SAINT software. The crystal structures were solved by the direct method and refined with full matrix least-squares on F^2 using SHELX-2015 (Sheldrick, 2015). The program SADABS (Bruker, 2016/2) was employed to correct the data for the effects of absorption. Nonhydrogen atoms were refined with anisotropic displacement parameters, and all hydrogen atoms were placed in the calculated positions and refined with a riding model. DIAMOND and PLATON software were utilized to generate figures and analyze the interactions of the potential hydrogen bonds, respectively.

Chemical Stability Experiment

Prior to studying the thermal effect on the chemical stability of GBP, GBP-2,6PDA salt and GBP-2,5PDA cocrystal, all of the samples were sieved through 140-mesh sieves but retained in the 200-mesh sieves to minimize the particle size effect. A total of 6.0 mg of GBP and 11.85 mg of GBP-2,5PDA cocrystal or GBP-2,6PDA salt were spread into 10-mL glass vials without lids and stored under 80℃/0% RH conditions for 27 days in a desiccator containing anhydrous calcium chloride ($CaCl_2$).

To test the degradation of GBP, GBP-2,6PDA salt and GBP-2,5PDA cocrystals under mechanical stress, the samples were milled in a planetary ball mill (XQM-0.2, Changsha, China) with four stainless steel balls (8 mm × 8.0 g) and a 16:1 (w/w) ratio of ball to materials. The milling experiments were conducted for 30 or 60 min at ambient temperature, and the milling speed was 800 rpm. After milling, 6.0 mg of the milled GBP and 11.85 mg of milled GBP-2,5PDA cocrystal or GBP-2,6PDA salt were placed into glass vials (10 mL) and stored in a desiccator containing anhydrous calcium chloride ($CaCl_2$) under 60℃/0% RH. The samples were removed at different time points and analyzed by PXRD to test the physical stability.

High Performance Liquid Chromatography (HPLC) Analysis

HPLC was applied to determine the remaining contents of GBP at different time points under thermal and mechanical stress. All tests were performed in triplicate. The concentrations of GBP were determined using a Shimadzu LC-20AT HPLC system (Shimadzu Corporation, Kyoto, Japan) with a UV detector at 210 nm. An Agilent SB-Zorbax C_{18} reversed-phase column (4.6 × 250 mm, 5 μm) was used to separate the components at 30℃. An isocratic method was applied with 70% buffer (95% 10 mM KH_2PO_4 and K_2PO_4, and 5% acetonitrile) and 30% methanol at a flow rate of 0.8 mL/min [3, 12].

Results and Discussion

Thermal Analysis

Thermal analysis of GBP, GBP-2,6PDA salt and GBP-2,5PDA cocrystal were conducted by DSC and TGA. The

DSC traces of GBP, coformers (2,5-PDA/2,6-PDA), GBP-2,6PDA salt and GBP-2,5PDA cocrystal are shown in Fig. 1. The melting points (T_{onset}) of the GBP, GBP-2,6PDA salt and GBP-2,5PDA cocrystal were 165.0℃, 168.2℃ and 152.5℃, respectively (Fig. 1a and 1b). The melting point of the GBP-2,6PDA salt was found to be between the values of GBP and 2,6PDA. The melting point of GBP-2,5PDA cocrystal was lower than those of the drug and coformer. There are few reported cocrystals showing lower melting points than the individual components [24, 25]. According to the TGA analysis (Fig. 1c and 1d), no weight loss occurred before 165℃, indicating that the formation of GBP-2,6PDA salt and GBP-2,5PDA cocrystal were not solvates or hydrates.

Powder X-ray Diffraction (PXRD)

The formation of new solid forms was verified by PXRD. Both the GBP-2,6PDA salt and GBP-2,5PDA cocrystal exhibited unique PXRD patterns compared to the individual components (Fig. 2). For GBP-2,6PDA salt, new diffraction peaks at 8.8°, 16.6°, 18.3° and 26.0° (2θ) were observed. The characteristic diffraction peaks of the GBP-2,5PDA cocrystals were 8.8°,19.3°, and 26.8° (2θ). All peaks presented in the PXRD patterns are consistent with those in the simulated patterns generated from the single-crystal structures, suggesting the formation of highly pure crystalline phases.

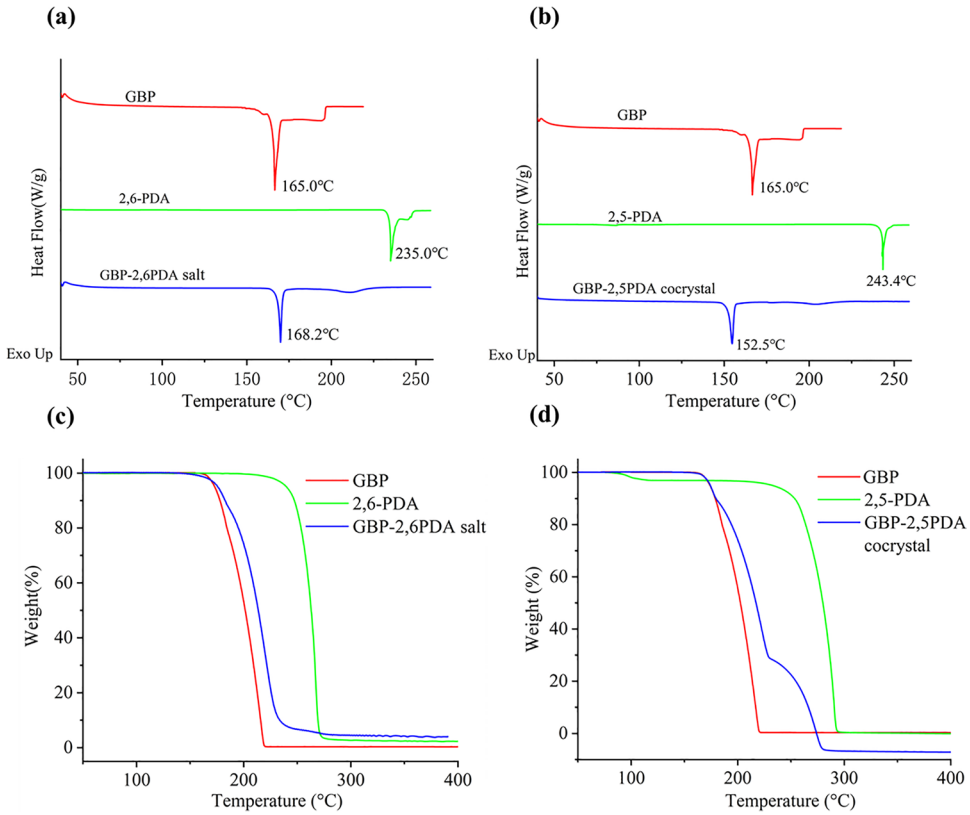

Fig. 1 Thermal analyses of GBP, 2,5-PDA, 2,6-PDA, GBP-2,6PDA salt and GBP-2,5PDA cocrystal: (**a**) and (**b**) DSC traces; (**c**) and (**d**) TGA traces.

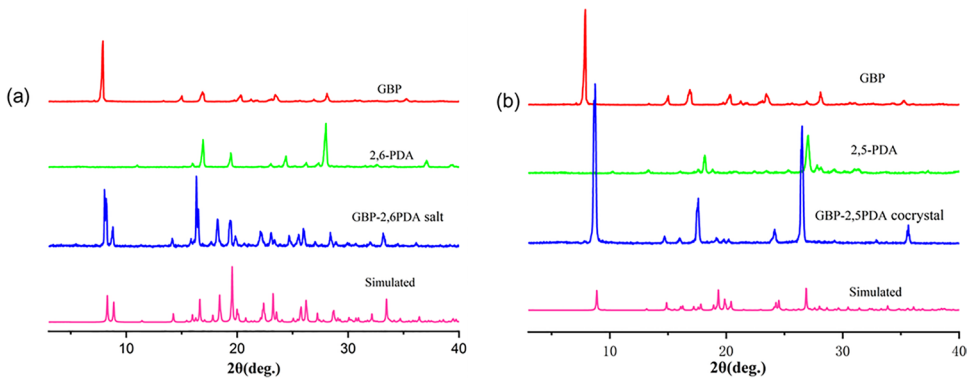

Fig. 2 (**a**) PXRD patterns of GBP, 2,6-PDA, GBP-2,6 PDA salt and simulated patterns from crystal structure, and (**b**) PXRD patterns of GBP, 2,5-PDA, GBP-2,5 PDA cocrystal and simulated patterns from crystal structure.

Single Crystal Structure Analysis

High-quality single crystals of GBP-2,6PDA salt and GBP-2,5PDA cocrystal were obtained as prismatic shapes by solvent evaporation (Fig. 3). The crystallographic data and hydrogen-bond geometries of the GBP-2,6PDA salt and GBP-2,5PDA cocrystal are listed in Tables 1 and S1-S2. The GBP-2,6PDA salt crystallized in the monoclinic $P2_1/c$ space group with one molecule of GBP and 2,6-PDA in the asymmetric unit (Table 1 and Fig. S1). In the GBP-2,5PDA cocrystal, GBP and 2,5PDA crystallized in the $P2_1/n$ space group with an asymmetric unit containing one GBP zwitterion and one 2,5-PDA molecule (Table 1 and Fig. S1).

The crystal arrangement and hydrogen-bonded network of the GBP-2,6PDA salt are shown in Fig. 4. To determine the ionization state of GBP molecules in the crystal structure of GBP-2,6PDA, the C-O bond lengths in the carboxylic group of 2,6PDA were examined. The neutral carboxylic acid C-O bond lengths may typically differ by more than 0.08 Å. However, for GBP-2,6PDA, the difference in C-O bond lengths in the carboxylic group was 0.01 Å, suggesting the proton transfer from 2,6-PDA to gabapentin to form a molecular salt [26, 27]. As shown in Fig. 4a, GBP interacted with 2,6-PDA via two supramolecular heterosynthons of $R_1^2(5)$ and $R_2^2(7)$ through N2-H2B···O2 (2.00 Å), N2-H2A···O3 (2.18 Å) and N2-H2B···N1 (2.34 Å) in the asymmetric unit. The motif of the GBP-2,6PDA salt was further extended by means of C9-H9B···O1 (2.49 Å), O4-H4···O2 (1.80 Å) and O5-H5···O1 (1.73 Å) hydrogen bonds, forming a "zigzag" chain along the *c* axis (Fig. 4b and Fig. 4c). Along the *b* axis, the "zigzag" chains were parallel to each other and stacked in a reverse orientation, forming a layered structure (Fig. 4d). There was no further hydrogen bonding nor π···π interactions between each "zigzag" chain.

The crystal packing and hydrogen-bonding interactions of the GBP-2,5PDA cocrystal was shown in Fig. 5. The difference in C-O bond lengths in the carboxylic group was greater than 0.08 Å, suggesting no proton transfer from 2,5-PDA to gabapentin. As shown in Fig. 5a, each GBP connected with 2,5-PDA through hydrogen bonds of N2-H2C···O2 (2.55 Å), N2-H2C···N1 (2.05 Å), N2-H2A···O1 (2.11 Å), C9-H9B···O1 (2.59 Å) and C10-H10A···O2 (2.59 Å). The asymmetric unit was linked to the adjacent unit through the hydrogen bonding of C4-H4A···O5 (2.51 Å) and C10-H10B···O3 (2.59 Å), resulting in a layered

Table 1 Crystallographic data for GBP salt/cocrystal

	GBP-2,6PDA salt	GBP-2,5PDA cocrystal
CCDC	2,168,329	2,168,337
Chemical formula	$C_{16}H_{22}N_2O_6$	$C_{16}H_{22}N_2O_6$
Crystal system	monoclinic	monoclinic
Formula weight	338.35	338.35
Space group	$P2_1/c$	$P2_1/n$
Temperature (K)	170	173
a (Å)	6.5439(6)	11.9006(6)
b (Å)	21.304(2)	7.2112(4)
c (Å)	11.3475(10)	18.5064(9)
α (deg)	90	90
β (deg)	97.016(3)	90.790(2)
γ (deg)	90	90
Volume (Å^3)	1570.1(2)	1588.02(14)
Z	4	4
ρ_{calc} (g/cm^3)	1.431	1.415
Λ (Mo-Kα)	0.71073	0.71073
μ (mm^{-1})	0.110	0.109
Crystal size (mm^3)	0.16×0.12×0.08	0.18×0.15x 0.12
R(int)	0.0804	0.0613
F(000)	720.0	720.0
θ range (°)	5.264–52.956	6.064–55.026
S	1.025	1.032
R_1, wR_2 [$I>2\sigma(I)$]	0.0572, 0.1282	0.0484, 0.1012
R_1, wR_2 (all data)	0.1034, 01,560	0.0827, 0.1198

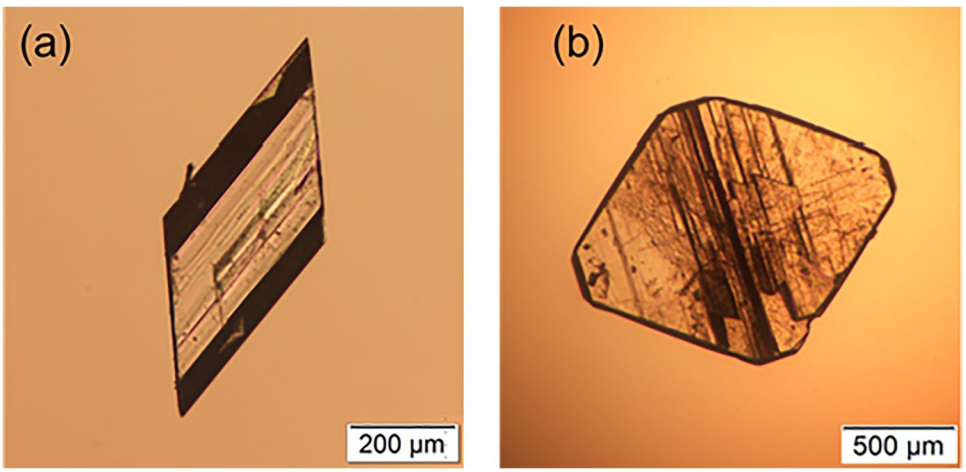

Fig. 3 Polarizing microscopy pictures for Polarizing microscopy images: (**a**) GBP-2,6PDA salt. and (**b**) GBP-2,5PDA cocrystal.

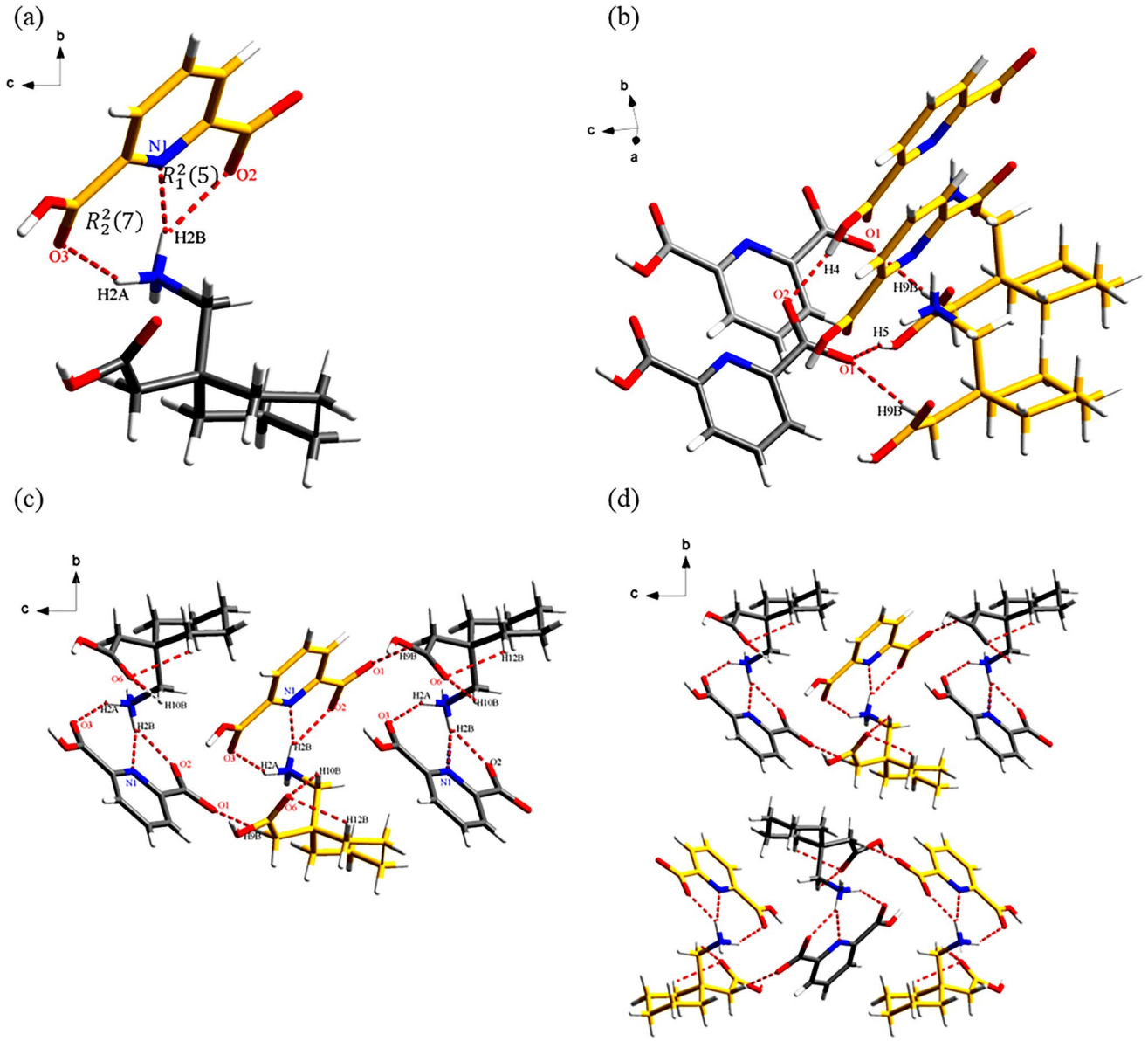

Fig. 4 **(a)** Partial hydrogen bond interactions of GBP-2,6PDA salt in the asymmetric unit; **(b)** and **(c)** hydrogen bonds connect between adjacent asymmetric units in GBP-2, 6PDA salt; **(d)** orientation of antiparallel chain in GBP-2, 6PDA salt.

structure (Fig. 5b). Along the *b* axis, the GBP molecule in one layer interacted with GBP in adjacent layers through the N2-H2B···O6 (1.92 Å) hydrogen bond to create a bilayer structure of the GBP-2,5PDA cocrystal (Fig. 5c). The neighboring bilayers were stacked together to produce a 3D structure (Fig. 5d).

Stability Under Thermal Stress

It has been reported that the lactamization rate of GBP can be accelerated by increasing the temperature [13]. To test the thermal stability of pure GBP, GBP-2,5PDA cocrystal and GBP-2,6PDA salt, the samples were stored in open vials under 80℃/0% RH for 27 days. The remaining contents of GBP in the different solid forms after thermal stress were determined by HPLC, and the results are summarized in Fig. 6. After 27 days, undesirable degradation was observed for pure GBP and the purity of GBP dropped to 92%. Unexpectedly, for the GBP-2,5PDA cocrystal, the content of GBP decreased to 90% after 27 days of storage, which dropped more rapidly compared to the neat GBP. In contrast, no significant degradation was observed for the GBP-2,6PDA salt after 27 days, and the content of GBP remained at 99%. The order of chemical stability under thermal stress was GBP-2,6PDA salt > GBP > GBP-2,5PDA cocrystal, showing that GBP-2,6PDA salt displayed superior chemical stability compared to the neat GBP and the 2,5PDA cocrystal.

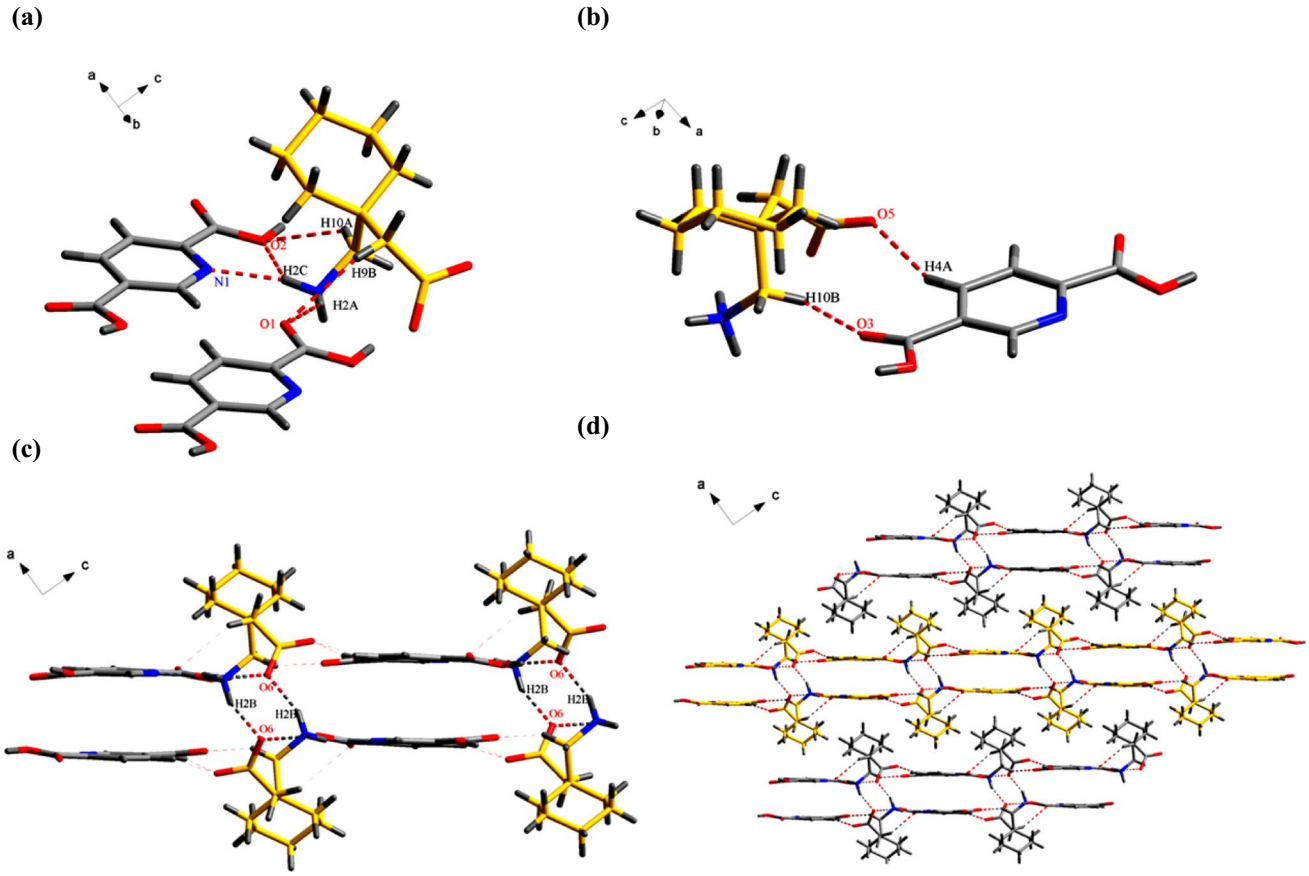

Fig. 5 (**a**) Partial hydrogen bond interactions of GBP-2,5PDA cocrystal in the asymmetric unit; (**b**) the hydrogen bonds between the adjacent asymmetric units in GBP-2,5PDA cocrystal; (**c**) the hydrogen bonds between GBP and 2,5-PDA in each bilayer; (**d**) the structure of layers in GBP-2,5PDA cocrystal.

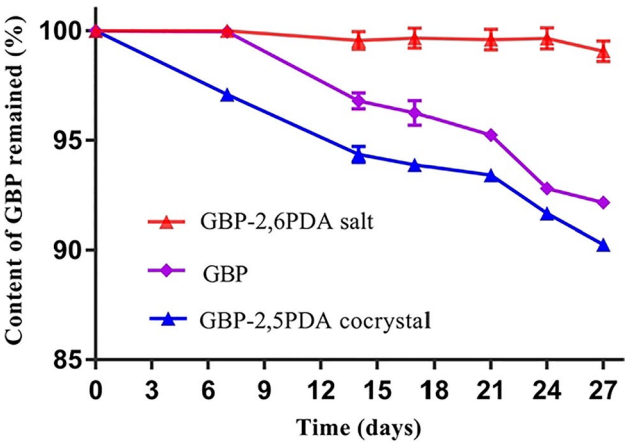

Fig. 6 Remaining content of GBP in samples of GBP, GBP-2,5PDA cocrystal and GBP-2,6PDA salt during storage at 80℃/0% RH for 27 days. (data are shown as mean ± SD, n = 3).

Stability Under Mechanical Stress

Crystalline GBP may easily undergo disordering under mechanical forces, leading to a higher tendency to degrade [12, 13]. In this study, we evaluated the impact of mechanical stress on the chemical stability of GBP, GBP-2,6PDA salt and GBP-2,5PDA cocrystal. The crystalline powders were milled in a planetary ball mill for 30 or 60 min. After milling, the samples were immediately transferred to open vials and exposed to storage conditions of 60℃/0% RH for 15 days. Samples were periodically removed for the stability test by HPLC and PXRD. As shown in Fig. 7, the PXRD patterns of unmilled and milled samples of GBP and its cocrystal/salt remained the same at different storage times, suggesting no phase transformation occurred during 15 days.

The remaining contents of GBP during storage are shown in Fig. 8. No obvious degradation of GBP was observed for any of samples immediately after milling (t = 0). However, the pure GBP crystal and GBP-2,5PDA cocrystal started to degrade during storage, while the GBP-2,6PDA salt remained stable over time. It was found that the longer milling time would trigger more drug degradation during the storage. Compared to the samples milled for 30 min, more degradations were observed for the neat GBP and the cocrystal milled for 60 min. Longer milling can increase the specific surface area and introduce more

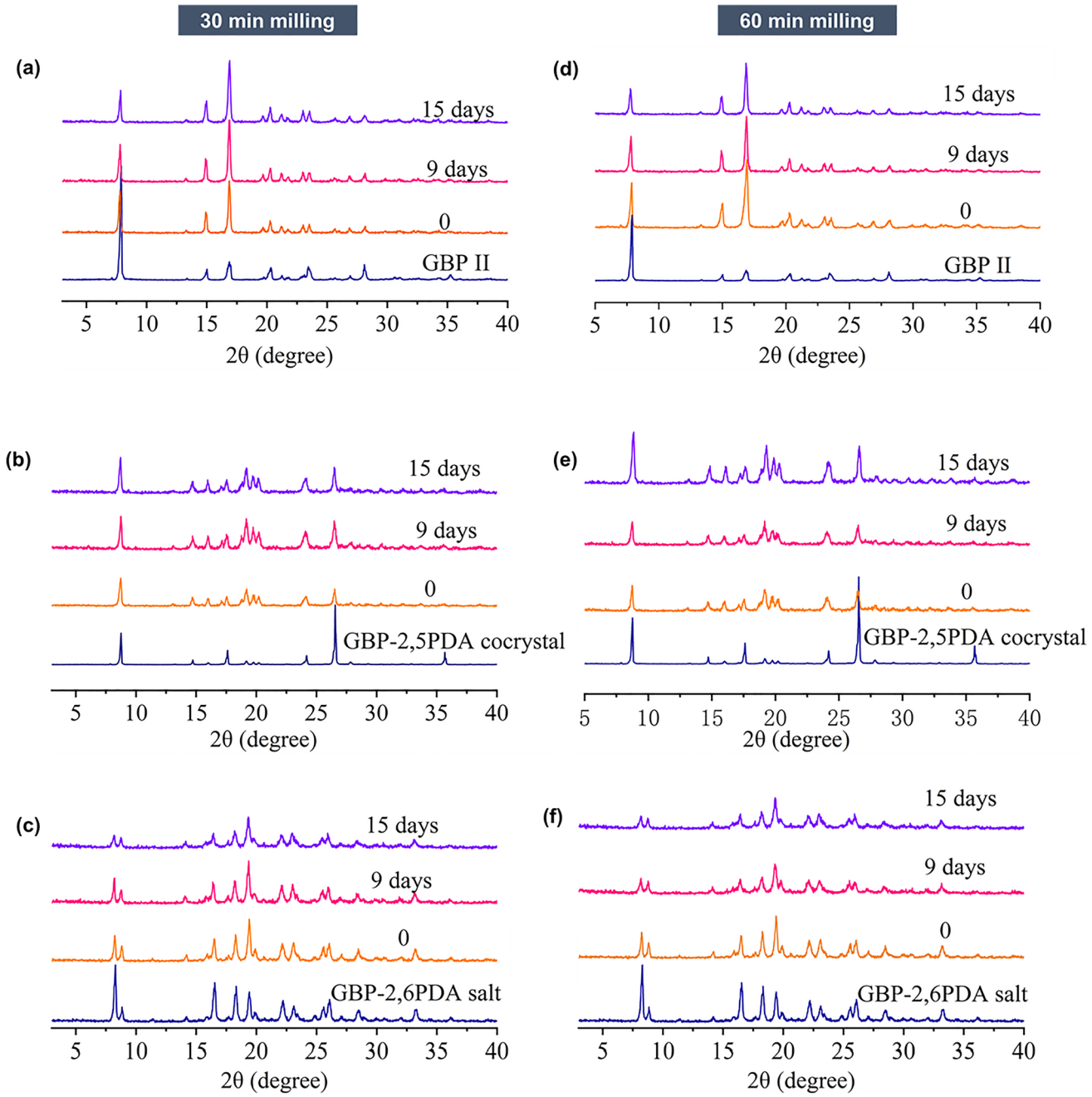

Fig. 7 PXRD patterns of milled samples during storage at 60℃/0% RH: 30 min milled samples (**a**) GBP II, (**b**) GBP-2,5PDA cocrystal and (**c**) GBP-2,6PDA salt; 60 min milled samples (**d**) GBP II, (**e**) GBP-2,5PDA cocrystal and (**f**) GBP-2,6PDA salt. Note: the 0 means the milled sample without storage.

defects and amorphous disorders at the surface of solids, which may lead to enhanced molecular mobility and reduced activation energy for the chemical degradation in the solid state. For the samples milled for 60 min, only 96.0% and 92.1% of GBP remained in the neat GBP and GBP-2,5PDA cocrystal after 15 days, respectively. Conversely, GBP-2,6PDA salt was quite stable after milling for 60 min, and no significant degradation was observed during storage. The rank order of the chemical stability under mechanical stress was GBP-2,6PDA salt > GBP > GBP-2,5PDA cocrystal.

Mechanism of Tuning the GBP Stability

The main degradation pathway of gabapentin is intramolecular condensation (i.e., lactamization). When the amino group approaches the carboxylic acid, the lone pair of electrons on the nitrogen atom may attack the carbonyl carbon

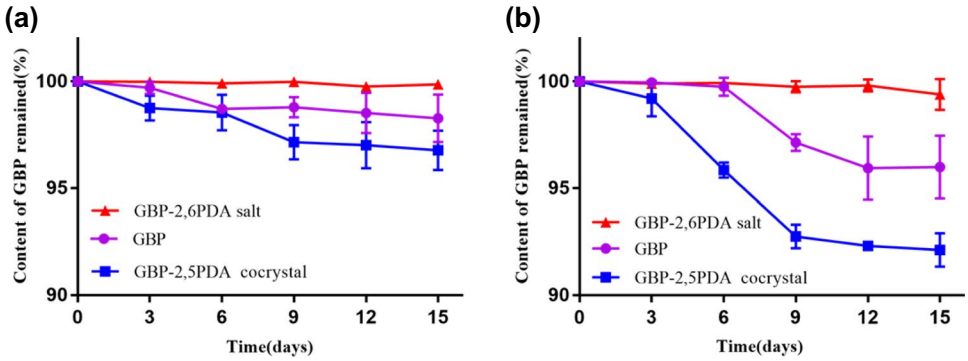

Fig. 8 Remaining content of GBP in the milled samples of GBP, GBP-2,5PDA cocrystal and GBP-2,6PDA salt during storage at 60℃/0% RH for 15 days (**a**) 30 min milled and (**b**) 60 min milled. (data are shown as mean ± SD, n = 3).

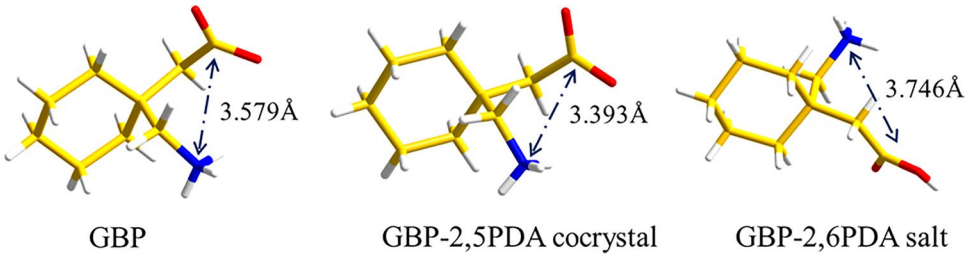

Fig. 9 Comparison of distances between C7 and N12 in the structures of GBP, GBP-2,5PDA cocrystal and GBP-2,6PDA salt.

to form the intermediate I, followed by a dehydration reaction to yield lactam product II (Scheme 1). Compared to other γ-amino carboxylic acids, gabapentin is a special case since the beta carbon is involved in the cyclohexane ring. Hence, the gem-dimethyl effect "pushes" the carboxylic and amino groups toward the same side, facilitating lactamization [28]. Therefore, we believe that the distance between the amino and carboxylic groups of GBP in the crystalline state may be the key factor influencing the chemical stability of GBP solids. Therefore, the distances between C7 and N12 of GBP in the crystal structure of different solid forms were determined by using Mercury software. As shown in Fig. 9, the distance of the reactive groups (C7 and N12) in the structure of the GBP-2,5PDA cocrystal (3.393 Å) is shorter than that of the neat GBP (3.579 Å), resulting in the accelerated degradation of GBP under thermal and mechanical stresses. Conversely, the distance between the $-NH_3^+$ and $-COO^-$ groups in the structure of the GBP-2,6PDA salt (3.746 Å) is significantly longer than those in the neat GBP and the cocrystal, leading to enhanced chemical stability. Furthermore, the electronic properties of the COO^- moiety is also changed in GBP-2,6PDA salt, which can affect the reactivity of the condensation process.

Conclusion

We successfully improved the chemical stability of the anticonvulsant drug Gabapentin (GBP) via crystal engineering. By incorporating another component into the crystal lattice, the molecular packing arrangement and the hydrogen bonding network were altered. Compared to the neat GBP and GBP-2,5PDA cocrystal, the formation of GBP-2,6PDA salt significantly improved the chemical stability of GBP under thermal and mechanical stress. The relationship between the chemical stability and crystal structures of GBP solids revealed that the distance between the carboxyl group (C7) and amino group (N12), the reaction active sites leading to dehydration condensation reaction of GBP, is a critical factor affecting the chemical stability of solid-state GBP. These findings proved that crystal engineering is a powerful strategy to enhance the chemical stability of unstable pharmaceutical solids during the manufacturing process and storage.

Supplementary Information The online version contains supplementary material available at https://doi.org/10.1007/s11095-022-03326-7.

Funding The authors are grateful for the financial support to this work from the National Natural Science Foundation of China (No. 81872813, 22108313), the Outstanding Youth Fund of Jiangsu Province of China (BK20190029), Natural Science Foundation of Jiangsu Province (BK 20200576), Fundamental Research Funds for the Central Universities (No 2632022ZD16) and the Program of State Key Laboratory of Natural Medicines-China Pharmaceutical University (No. SKLNMZZ202031).

Declarations

Conflict of Interest The authors have no conflicts of interest to declare.

References

1. Goa KL, Sorkin EM. Gabapentin Drugs. 1993;46(3):409–27.
2. Dobecki DA, Schocket SM, Wallace MS. Update on Pharmacotherapy Guidelines for the Treatment of Neuropathic Pain. Curr Pain Headache Rep. 2006;10(3):185–90.
3. Wang J, Yang L, Li D, Xu Y, Yang L, Zhao H, Zhu Z, Luan H, Luo Q. Investigating the Mechanism of L-Valine in Improving the Stability of Gabapentin Combining Chemical Analysis Experiments with Computational Pharmacy. AAPS PharmSciTech. 2019;20(3):114.
4. McLean MJ, Gidal BE. Gabapentin Dosing in the Treatment of Epilepsy. Clin Ther. 2003;25(5):1382–406.
5. Sills GJ. The Mechanisms of Action of Gabapentin and Pregabalin. Curr Opin Pharmacol. 2006;6(1):108–13.
6. Baastrup C, Finnerup NB. Pharmacological Management of Neuropathic Pain Following Spinal Cord Injury. CNS Drugs. 2008;22(6):455–75.
7. Hagen EM, Rekand T. Management of Neuropathic Pain Associated with Spinal Cord Injury. Pain Ther. 2015;4(1):51–65.
8. Kukkar A, Bali A, Singh N, Jaggi AS. Implications and Mechanism of Action of Gabapentin in Neuropathic Pain. Arch Pharm Res. 2013;36(3):237–51.
9. Hadidi S, Shiri F, Norouzibazaz M. Theoretical Mechanistic Insight into the Gabapentin Lactamization by an Intramolecular Attack: Degradation Model and Stabilization Factors. J Pharm Biomed Anal. 2020;178: 112900.
10. Dempah KE, Barich DH, Kaushal AM, Zong Z, Desai SD, Suryanarayanan R, Kirsch L, Munson EJ. Investigating Gabapentin Polymorphism Using Solid-State Nmr Spectroscopy. AAPS PharmSciTech. 2013;14(1):19–28.
11. Lin S, Hsu C, Ke W-T. Solid-State Transformation of Different Gabapentin Polymorphs Upon Milling and Co-Milling. Int J Pharm. 2010;396(1):83–90.
12. Zong Z, Desai SD, Kaushal AM, Barich DH, Huang H, Munson EJ, Suryanarayanan R, Kirsch LE. The Stabilizing Effect of Moisture on the Solid-State Degradation of Gabapentin. AAPS PharmSciTech. 2011;12(3):924–31.
13. Zong Z, Qiu J, Tinmanee R, Kirsch LE. Kinetic Model for Solid-State Degradation of Gabapentin. J Pharm Sci. 2012;101(6):2123–33.
14. Augart H, Gebhardt UWE, Herrmann W. Lactam-Free Amino Acids. U.S. Patent 6054482 [A]. 2000-04-25.
15. Coetzee JF, Mosher RA, Kohake LE, Cull CA, Kelly LL, Mueting SL, KuKanich B. Pharmacokinetics of Oral Gabapentin Alone or Co-Administered with Meloxicam in Ruminant Beef Calves. Vet J. 2011;190(1):98–102.
16. Guo M, Sun X, Chen J, Cai T. Pharmaceutical Cocrystals: A Review of Preparations, Physicochemical Properties and Applications. Acta Pharm Sin B. 2021;11(8):2537–64.
17. Yang D, Wang H, Liu Q, Yuan P, Chen T, Zhang L, Yang S, Zhou Z, Lu Y, Du G. Structural Landscape on a Series of Rhein: Berberine Cocrystal Salt Solvates: The Formation, Dissolution Elucidation from Experimental and Theoretical Investigations. Chin Chem Lett. 2022;33(6):3207–11.
18. Wang J, Zhou C, Yu X, Mei X. Stabilizing Vitamin D3 by Conformationally Selective Co-Crystallization. Chem Commun. 2014;50(7):855–8.
19. Yu Q, Yan Z, Bao J, Wang J, Mei X. Taming Photo-Induced Oxidation Degradation of Dihydropyridine Drugs through Cocrystallization. Chem Commun. 2017;53(91):12266–9.
20. Li M, Li Z, Zhang Q, Peng B, Zhu B, Wang J, Liu L, Mei X. Fine-Tuning the Colors of Natural Pigment Emodin with Superior Stability through Cocrystal Engineering. Cryst Growth Des. 2018;18(10):6123–32.
21. Liu L, Wang J, Mei X. Enhancing the Stability of Active Pharmaceutical Ingredients by the Cocrystal Strategy. CrystEngComm. 2022;24(11):2002–22.
22. Reddy LS, Bethune SJ, Kampf JW, Rodríguez-Hornedo N. Cocrystals and Salts of Gabapentin: Ph Dependent Cocrystal Stability and Solubility. Cryst Growth Des. 2009;9(1):378–85.
23. Wenger M, Bernstein J. An Alternate Crystal Form of Gabapentin: A Cocrystal with Oxalic Acid. Cryst Growth Des. 2008;8(5):1595–8.
24. Huang S, Xue Q, Xu J, Ruan S, Cai T. Simultaneously Improving the Physicochemical Properties, Dissolution Performance, and Bioavailability of Apigenin and Daidzein by Co-Crystallization with Theophylline. J Pharm Sci. 2019;108(9):2982–93.
25. Chadha K, Karan M, Bhalla Y, Chadha R, Khullar S, Mandal S, Vasisht K. Cocrystals of Hesperetin: Structural, Pharmacokinetic, and Pharmacodynamic Evaluation. Cryst Growth Des. 2017;17(5):2386–405.
26. Aakeröy CB, Rajbanshi A, Li ZJ, Desper J. Mapping out the Synthetic Landscape for Re-Crystallization. Co-Crystallization and Salt Formation CrystEngComm. 2010;12(12):4231–9.
27. Tao Q, Hao Q, Voronin AP, Dai X, Huang Y, Perlovich GL, Lu T, Chen J. Polymorphic Forms of a Molecular Salt of Phenazopyridine with 3,5-Dihydroxybenzoic Acid: Crystal Structures, Theoretical Calculations, Thermodynamic Stability, and Solubility Aspects. Cryst Growth Des. 2019;19(10):5636–47.
28. Jung ME, Piizzi G. Gem-Disubstituent Effect: Theoretical Basis and Synthetic Applications. Chem Rev. 2005;105(5):1735–66.